Materials Research Bulletin 73 (2016) 153–163

Contents lists available at ScienceDirect

Materials Research Bulletin

journal homepage: www.elsevier.com/locate/matresbu

Cr-substitution effect on structural, optical and electrical properties of $Cr_xCe_{1-x}PO_4$ ($x = 0.00$, 0.08, 0.10 and 0.20) nanorods

Amor Fadhalaoui[a], Hassouna Dhaouadi[b,*], Houda Marouani[a], Abdessalem Kouki[c], Adel Madani[d], Mohamed Rzaigui[a]

[a] Laboratoire de Chimie des Matériaux, Faculté des Sciences de Bizerte, Zarzouna, Bizerte 7021, Tunisia
[b] Laboratoire Matériaux Traitement et Analyse, INRAP, Technopôle Sidi-Thabet, Tunis 2020, Tunisia
[c] L3M, FSB, Zarzouna, Bizerte 7021, Tunisia
[d] Department of Physics, Applied Science College, Umm Al Qura University, Makkah, Saudi Arabia

ARTICLE INFO

Article history:
Received 28 March 2015
Received in revised form 14 July 2015
Accepted 18 August 2015
Available online 14 September 2015

Keywords:
A. Nanostructures
B. Chemical synthesis
C. Impedance spectroscopy
C. X-ray diffraction
C. Transmission electron microscopy (TEM)

ABSTRACT

$Cr_xCe_{1-x}PO_4$ ($x = 0.00–0.20$) nanorods were synthesized using the hydrothermal method. The as-prepared samples were characterized by X-ray diffraction (XRD), infrared absorption spectroscopy (IR) and transmission electron microscopy (TEM). The XRD results revealed the formation of a pure $CePO_4$ hexagonal phase. TEM images confirmed the nano-size character of the as-prepared samples. Impedance spectroscopy analysis was used to analyze the electrical behavior of samples as a function of frequency at different temperatures. The increase of Cr-amount led to an increase in the total conductivities and decreased the activation energies (E_a ($x = 0.00$) = 1.08 eV to E_a ($x = 0.20$) = 0.80 eV). The optical properties of $Cr_xCe_{1-x}PO_4$ nanomaterials were investigated using UV–vis spectroscopy. The band-gap energy values decreased with increasing Cr-content showing a red-shift trend. The improvement of the electrical conductivity and optical properties makes the $Cr_xCe_{1-x}PO_4$ nanomaterials possible candidates to be used as electrolytes in solid oxide fuel cells, in photocatalytic and photovoltaic applications.

1. Introduction

Cerium orthophosphates have been the subject of intense research in the past few years, mainly due to their use in the production of moisture sensors for luminescent materials, heat resistant materials and hosts for radioactive nuclear waste [1].

Many studies concerning the microstructure and optical properties of $CePO_4$ nano-materials have been published [1]. In previous work on cerium orthophosphate [2], detailed studies using impedance analysis spectroscopy have been carried out on its synthesis, its electrical conductivity and dielectric properties. Doping $CePO_4$ with trivalent rare earth ions resulted in different morphologies, sizes and improved physico-chemical properties [1]. Many attempts have been made to study and improve the electrical conductivity of (La,Ce)PO_4 by a Ca and Sr-doping process [3–4]. In this work, the effect of doping by Cr^{3+} ions on the structural, optical and electrical properties of the same rare earth Phosphate $CePO_4$ is presented. However, the exact substitution effect depends on the nature of the doping elements. The chromium element has the stability of the (+III) valence state in reducing conditions, and is exploited in the *p*-type conducting SOFC interconnect materials [5]. Many reports reveal that substitution with paramagnetic Cr^{3+} ions introduces magnetic dilution in ferrites similar to that produced by non-magnetic substitution which may induce interesting properties in ferrites [6–7]. The partial substitution of Fe^{3+} by Cr^{3+} in $LiCr_yFe_{1-y}P_2O_7$ and its use as a positive electrode material seems to be a convenient way of reducing the oxidation potential which is essential for electrolyte stability [8]. The Cr-doping of $CePO_4$ is expected to improve its optical and electrical properties.

In this study $Cr_xCe_{1-x}PO_4$ ($x = 0.00$, 0.08, 0.10 and 0.20) nanorods were synthesized for the first time. To the best of our knowledge the Cr-substitution effect on the structural and electrical properties of $CePO_4$ ceramic materials has not been previously investigated. In addition, this study aims to correlate the structural changes of the as-prepared material with the Cr^{3+} ion content using the FTIR, XRD and TEM techniques. Obvious improvements to the electrical conductivity and the optical properties were achieved compared to the undoped $CePO_4$.

---

* Corresponding author. Fax: +216 71 537 688.
E-mail address: dhaouadihassouna@yahoo.fr (H. Dhaouadi).

http://dx.doi.org/10.1016/j.materresbull.2015.08.018
0025-5408/

2. Experimental

Stoichiometric molar ratios of $CeCl_3 \cdot 7H_2O$ and $CrCl_3 \cdot 7H_2O$ were dissolved in 20 mL of distilled water under continuous stirring. A calculated quantity of PEG-8000 was added to the suspension. A calculated amount of H_3PO_4 was then added to the homogenous solution and continuously stirred for 1 h. The mixture was then transferred into a 100 mL Teflon-lined stainless steel autoclave. The autoclave was sealed and heated at 150 °C for 3 h in an electric oven and left to cool down naturally to room temperature. The precipitates were collected by centrifugation and washed several times using ethanol and de-ionized water.

The XRD pattern was determined using a PANalytical XPERT PROMPD diffractometer operating with Cu Kα radiation ($\lambda = 0.15406$ nm). TEM studies were recorded on a JEOL 100-CX-II electron microscope operated at 200 kV. Fourier-transform infrared (FT-IR) spectra were obtained with a BRUKER Vertex-70 FTIR spectrometer. Raman spectroscopy was performed using a Jobin-Yvon T-64000 spectrometer. The UV–vis spectra were recorded on a Shimadzu UV3101PC visible spectrophotometer in the 200–800 nm range. Impedance spectroscopy measurements were taken for the compressed pellets of the $Cr_xCe_{1-x}PO_4$ samples. Conducting silver paste was applied to both sides of the pellets to serve as electrodes. Conductivity measurements were carried out from 360 to 460 °C in 20 °C intervals by checking the complex impedance spectroscopy with a Hewlett Packard 4129A impedance analyzer. The signal frequency ranged from 10 Hz to 13 MHz.

3. Results and discussion

3.1. X-ray study

Fig. 1 shows the X-ray patterns of $Cr_xCe_{1-x}PO_4$ prepared by the hydrothermal method. The XRD patterns indicate that all samples exhibit a single phase with a hexagonal-type structure (Reference code: 00-004-0632).

The observed broad peaks in Fig. 1 indicate the nanosize character of the as-prepared samples.

The weak steady shift towards higher angles and the observed decrease of the peak intensities could be explained by the larger ionic radii of Ce^{3+} ($r = 1.15$ Å) compared to that of Cr^{3+} ($r = 0.63$ Å) in a six-fold coordination environment. The small shift indicates that the doping of $CePO_4$ by Cr^{3+} ions does not have a considerable effect on the crystallographic parameters. The refined cell parameters of $Cr_xCe_{1-x}PO_4$ samples are shown in Table 1. From Table 1, we notice that the parameters and the lattice volume V decreased after increasing Cr-content. The existence of too many Cr ions may induce large changes in the structure and cause the instability phase. The slight shift of diffraction peaks to large angle was also observed when Fe^{3+} ion (0.645 Å) substitutes La^{3+} ion (1.061 Å) in $LaPO_4$ [9]. This implies that smaller Fe^{3+} ions could substitute bigger La^{3+} ions into phosphate lattice.

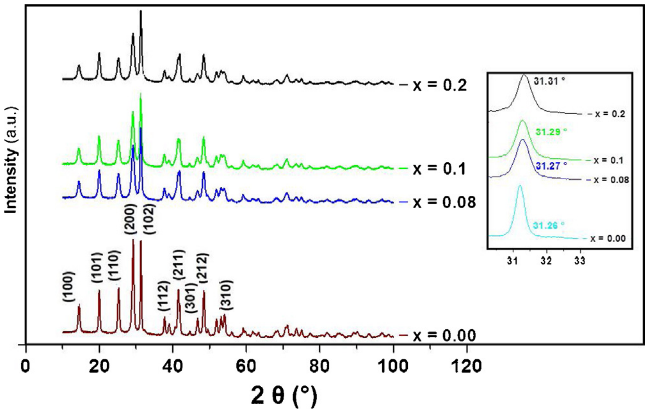

Fig. 1. XRD patterns of $Cr_xCe_{1-x}PO_4$ ($x = 0.00$, 0.08, 0.10 and 0.20) nanorods. (Inset) Shift of the Bragg reflections (2 0 0) for the different studied compositions.

The mean crystallite size estimated from Scherrer's formula was found to be: $D_0 = 29$ nm ($x = 0.00$), $D_{0.08} = 18.6$ nm ($x = 0.08$), $D_{0.1} = 17.0$ nm ($x = 0.10$) and $D_{0.2} = 14.6$ nm ($x = 0.20$) and was dependent on the chromium and cerium concentration.

This could be explained by the partial substitution effect of Cr^{3+} ions which causes the changes in the unit cell volume and consequently affects the particle size. The main reason for the decrease of the grain size may be due to the fact that doping introduced defects and the defects prevent grain to grow [10]. On the other hand, the doping elements may have low solid solubility with the original material and their accumulation in the grain boundary might have restrained the growth of the grain.

3.2. TEM characterization

TEM was used to study the effect of Cr-partial substitution on the particle size and shape of $Cr_xCe_{1-x}PO_4$. Representative TEM images of the final products as a function of the Cr-content clearly show the nanometer feature of the as-prepared samples (Fig. 2).

As seen from Fig. 2(a–d) for $Cr_xCe_{1-x}PO_4$ materials, all the products exhibited a nanorod morphology measuring a few hundred nanometers in length and 20–40 nm in width, which is in good agreement with the results of the XRD. Examining TEM images, it was found that the whole product takes on a similar shape to the nanorod morphology with the size depending on the Cr-content.

The particles have good dispersibility with little aggregation. This is mainly because the hydroxyl group of the PEG-8000 easily forms a hydrogen bond with the oxygen atoms. Once the nuclei have formed, PEG-8000 can easily adhere to the surface of the nuclei at the O-terminate through the hydrogen-bonding. During the crystal growth process, PEG-8000 influences the ordering manner of the crystal growth, leading to the change in crystal shape.

Thus, the PEG-8000 surfactant plays a crucial role in protecting the particles from rapid flocculation, thus inhibiting the agglomeration process. PEG-8000 acts as a capping agent and can exert a strong influence on the shape of as-formed particles by governing the growth rate of various crystallographic surfaces and create a favorable orientation in the nanocrystal formation. PEG-8000 was adsorbed on the crystal faces, which prevented the solute from diffusing onto the faces, so the crystal grew along one dimension to form $Cr_xCe_{1-x}PO_4$ nanorods as shown in Fig. 2. The use of PEG-8000 as surfactant can alter the nanoparticles' shape, size and other surface properties.

In order to study the surfactant effect on the morphology, $CePO_4$ was also prepared under the same hydrothermal conditions without using the PEG-8000 as surfactant. Broken and aggregated nanorods are obtained as seen in Fig. 2(e).

3.3. EDS analysis

The chemical analysis of the $Cr_xCe_{1-x}PO_4$ nanorods is determined by energy dispersive x-ray (EDX) analysis as shown in Fig. 3(a–e). The EDX analysis of the $Cr_xCe_{1-x}PO_4$ nanorods resulted in higher concentration of P, O and Ce elements and lower concentrations of Cr element. The EDX spectrums for $x = 0.08$, 0.1 and 0.2 showed the presence of Cr-peaks, determining the presence of this element in the material constitution. Therefore, the results have given evidence that Cr has been successfully incorporated into $CePO_4$. The C and Cu peaks come from the